

# Electroweak instantons/sphalerons at VLHC?

A. Ringwald

Deutsches Elektronen-Synchrotron DESY, Hamburg, Germany

## Abstract

There is a close analogy between electroweak instanton-induced baryon plus lepton number ( $B + L$ ) violating processes in Quantum Flavor Dynamics (QFD) and hard QCD instanton-induced chirality violating processes in deep-inelastic scattering. In view of the recent information about the latter both from lattice simulations and from the H1 experiment at HERA, it seems worthwhile to reconsider electroweak  $B + L$  violation at high energies. We present a state of the art evaluation of QFD instanton-induced parton-parton cross-sections, as relevant at future high energy colliders in the hundreds of TeV regime, such as the projected Very Large Hadron Collider (VLHC). We find that the cross-sections are unobservably small in a conservative fiducial kinematical region inferred from the above mentioned QFD–QCD analogy. An extrapolation – still compatible with lattice results and HERA – beyond this conservative limit indicates possible observability at VLHC.

1. The Standard Model of electroweak (Quantum Flavor Dynamics (QFD)) and strong (QCD) interactions is remarkably successful and describes quantitatively a wealth of data accumulated over the last decades. This success is largely based on the possibility to apply ordinary perturbation theory to the calculation of hard, short-distance dominated scattering processes, since the relevant gauge couplings are small.

There is, however, a class of processes which – even for small gauge couplings – can not be described by ordinary perturbation theory. These processes are associated with axial anomalies [1] and manifest themselves as anomalous violation of baryon plus lepton number ( $B + L$ ) in QFD and chirality ( $Q_5$ ) in QCD [2]. They are induced by topological fluctuations of the non-Abelian gauge fields, notably by instantons [3].

Such topological fluctuations and the anomalous processes induced by them are crucial ingredients for an understanding of a number of non-perturbative issues in the Standard Model. Indeed, QCD instantons have been argued to play an important role in various long-distance aspects of QCD, such as giving a possible solution to the axial  $U(1)$  problem [2] or being at work in  $SU(n_f)$  chiral symmetry breaking [4] (for reviews, see Ref. [5]). In QFD, on the other hand, similar topological fluctuations of the gauge fields and the associated  $B + L$  violating processes are very important at high temperatures [6] and have therefore a crucial impact on the evolution of the baryon and lepton asymmetries of the universe (see Ref. [7] for a review).

A very interesting, albeit unsolved question is whether manifestations of such topological fluctuations might be directly observable in high-energy scattering at present or future colliders (for a short review, see Ref. [8]). This question has been raised originally in the late eighties in the context of QFD [9, 10]. But, despite considerable theoretical [11, 12, 13, 14] and phenomenological [15, 16] efforts, the actual size of the cross-sections in the relevant, tens of TeV energy regime was never established (for reviews, see Refs. [7, 17]). Meanwhile, the focus switched to quite similar QCD instanton-induced hard scattering processes in deep-inelastic scattering [18, 19], which are calculable from first principles within instanton-perturbation theory [20], yield sizeable rates for observable final state signatures in the fiducial regime of the latter [21, 22, 23, 24], and are actively searched for at HERA [25]. Moreover, larger-size QCD instantons, beyond the semi-classical, instanton-perturbative regime, might well be responsible for the bulk of inelastic hadronic processes and build up soft diffractive scattering [26].

In view of the close analogy of QFD and hard QCD instanton-induced processes in deep-inelastic scattering [19], emphasized throughout this letter, and of the recent information about the latter both from lattice simulations [27, 22, 24] and from experiment [25], recalled and elaborated on below, it seems worthwhile to reconsider electroweak  $B+L$  violation at high energies. We therefore present in this letter a state of the art evaluation of QFD instanton-induced parton-parton cross-sections – quite analogous to the one presented in Ref. [21] for QCD instanton-induced processes –, as relevant at future high energy colliders in the hundreds of TeV regime, such as the projected Eurasian Long Intersecting Storage Ring (ELOISATRON) [28] or the Very Large Hadron Collider (VLHC) [29]. This goes along with a discussion of the implications of the lattice and HERA results – via the above mentioned QFD–QCD analogy – for the fate of electroweak  $B + L$  violation in high energy collisions.

2. QCD (QFD) instantons [3, 2] are (constrained [30]) minima of the classical Euclidean Yang-Mills action, localized in space and Euclidean time, with unit topological charge (Pontryagin index)  $Q = 1$ . In Minkowski space-time, instantons describe tunneling transitions between classically degenerate, topologically inequivalent vacua, differing in their winding number (Chern-Simons number) by one unit,  $\Delta N_{\text{CS}} = Q = 1$  [31]. The corresponding energy barrier (“sphaleron energy” [32]), under which the instantons tunnel, is inversely proportional to  $\alpha_g \equiv g^2/(4\pi)$ , the fine-structure constant of the relevant gauge theory, and the effective instanton-size  $\rho_{\text{eff}}$ ,

$$M_{\text{sp}} \sim \frac{\pi}{\alpha_g \rho_{\text{eff}}} \sim \begin{cases} \pi \frac{M_W}{\alpha_W} \sim 10 \text{ TeV} & \text{in QFD [32]}, \\ \mathcal{Q} & \text{in QCD [19, 20, 21]}, \end{cases} \quad (1)$$

where  $\mathcal{Q}$  is a large momentum transfer e.g. in deep-inelastic scattering (DIS), which should be taken  $\gtrsim 10 \text{ GeV}$  in order to be in the semi-classical, instanton-perturbative regime [20, 21, 22, 24]. As mentioned in Sect. 1, axial anomalies [1] force instanton-induced hard scattering processes to be always associated with anomalous fermion-number violation [2], in particular  $B + L$  violation,  $\Delta B = \Delta L = -n_{\text{gen}} Q$ , in the case of QFD with  $n_{\text{gen}} = 3$  fermion generations, and chirality violation,  $\Delta Q_5 = 2n_f Q$ , in the case of QCD with typically  $n_f = 3$  light quark flavors.

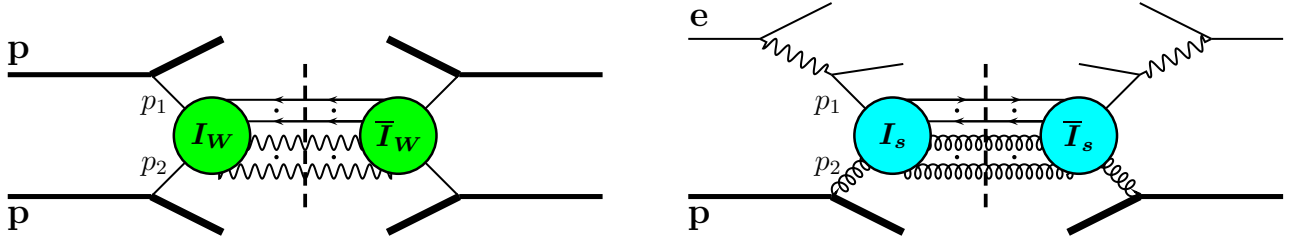


Figure 1: Illustration of a QFD instanton-induced process in proton-proton scattering (left) and of a QCD instanton-induced process in deep-inelastic electron-proton scattering (right).

Instanton-induced total cross-sections for hard parton-parton ( $p_1$ - $p_2$ ) scattering processes (cf. Fig. 1) are given in terms of an integral over the instanton-anti-instanton<sup>1</sup> ( $I\bar{I}$ ) collective coordinates (sizes  $\rho, \bar{\rho}$ ,  $I\bar{I}$  distance  $R$ , relative color orientation  $U$ ) [21] (see also [12, 13, 14, 33, 34])

$$\begin{aligned} \hat{\sigma}_{p_1 p_2}^{(I)} &\sim \frac{1}{2 p_1 \cdot p_2} \text{Im} \int d^4 R e^{i(p_1 + p_2) \cdot R} \\ &\times \int_0^\infty d\rho \int_0^\infty d\bar{\rho} D(\rho) D(\bar{\rho}) \int dU e^{-\frac{4\pi}{\alpha_g} \Omega\left(U, \frac{R^2}{\rho\bar{\rho}}, \frac{\bar{\rho}}{\rho}, \dots\right)} \left[ \omega\left(U, \frac{R^2}{\rho\bar{\rho}}, \frac{\bar{\rho}}{\rho}, \dots\right) \right]^{n_{\text{fin}}} \\ &\times F\left(\sqrt{-p_1^2} \rho\right) F\left(\sqrt{-p_1^2} \bar{\rho}\right) F\left(\sqrt{-p_2^2} \rho\right) F\left(\sqrt{-p_2^2} \bar{\rho}\right) \mathcal{P}_{p_1 p_2}^g(U, R, \rho, \bar{\rho}; p_1 \cdot p_2). \end{aligned} \quad (2)$$

Here, the basic blocks arising in instanton-perturbation theory – the semi-classical expansion of the corresponding path integral expression about the instanton solution – are *i*) the instanton-size distribution  $D(\rho)$ , *ii*) the function  $\Omega$ , which takes into account the exponentiation of gauge

<sup>1</sup>Both an instanton and an anti-instanton enter here, since we write the cross-section (2) as a discontinuity of the  $p_1 p_2$  forward elastic scattering amplitude in the  $I\bar{I}$ -background (cf. Fig. 1). Alternatively, one may calculate the cross-section by taking the modulus squared of amplitudes in the single instanton-background.

boson production [10, 12] and can be identified with the  $I\bar{I}$ -interaction defined via the valley method [35, 13, 36, 37], and *iii*) the function  $\omega$ , which summarizes the effects of final-state fermions. Their number  $n_{\text{fin}}$  is related to the number  $n_{\text{in}}$  of initial-state fermions via the anomaly,

$$n_{\text{fin}} + n_{\text{in}} \equiv n_{\text{tot}} \equiv \begin{cases} 4 n_{\text{gen}} = 12 & \text{in QFD,} \\ 2 n_f & \text{in QCD.} \end{cases} \quad (3)$$

With each initial-state parton  $p$ , there is an associated “form factor” [20, 21],

$$F(x) = x K_1(x) \begin{cases} \sim \sqrt{\pi/(2x)} \exp(-x) & \text{for } x \rightarrow +\infty, \\ = 1 & \text{for } x = 0. \end{cases} \quad (4)$$

The function  $\mathcal{P}_{\text{p1p2}}^g$  in Eq. (2) consists of further smooth factors [21], which will be included in our final result for the special case of QFD instantons below.

*Ad i)* The instanton-size distribution  $D(\rho)$  is known in instanton-perturbation theory,  $\alpha_g(\rho^{-1}) \ll 1$ , up to two-loop renormalization group invariance [2, 38, 39]. In QCD, the loop corrections are sizeable in the phenomenologically interesting range [21, 22]. However, for our illustrative purposes in this letter the one-loop expression for the size distribution,

$$D(\rho) = \frac{d}{\rho^5} \left( \frac{2\pi}{\alpha_g(\mu)} \right)^{2N_c} (\mu \rho)^{\beta_0} e^{-\frac{2\pi}{\alpha_g(\mu)} S^{(I)}}, \quad (5)$$

suffices, which, moreover, is numerically adequate for the case of QFD because of its weak coupling,  $\alpha_W(M_W) \equiv \alpha(M_W)/\sin^2 \hat{\theta}(M_W) = 0.033819(23)$  [40]. In Eq. (5),

$$\beta_0 = \frac{11}{3} N_c - \frac{1}{6} n_s - \frac{1}{3} n_{\text{tot}} = \begin{cases} 19/6 & \text{in QFD } (N_c = 2, n_s = 1, n_{\text{tot}} = 12), \\ 11 - 2n_f/3 & \text{in QCD } (N_c = 3, n_s = 0, n_{\text{tot}} = 2n_f), \end{cases} \quad (6)$$

denotes the first coefficient in the  $\beta$  function,

$$S^{(I)} = \begin{cases} 1 + \frac{1}{2} M_W^2 \rho^2 + \mathcal{O}(M_W^4 \rho^4 \ln(M_W \rho)) & \text{in QFD [2, 30],} \\ 1 & \text{in QCD [3],} \end{cases} \quad (7)$$

the instanton action,  $\mu$  the renormalization scale, and  $d$  a scheme-dependent constant, which reads in the  $\overline{\text{MS}}$  scheme [41],

$$d_{\overline{\text{MS}}} = \frac{2 e^{5/6}}{\pi^2 (N_c - 1)!(N_c - 2)!} e^{-1.511374 N_c + 0.291746 (n_{\text{tot}} + n_s)/2}. \quad (8)$$

The validity of instanton-perturbation theory, on which the prediction of the instanton-induced subprocess cross-section (2) is based, requires instantons of small enough size,  $\alpha_g(\rho^{-1}) \ll 1$ . In QFD, this is guaranteed by the exponential decrease  $\propto \exp(-\pi M_W^2 \rho^2 / \alpha_W)$  (cf. (7)) of the size distribution (5) for  $\rho > \rho_{\text{max}} \equiv \sqrt{\beta_0 \alpha_W / (2\pi)} / M_W = 0.13 / M_W$  (cf. Fig. 2 (left)). Therefore, the relevant contributions to the size integrals in (2) arise consistently from the perturbative region ( $\alpha_W(\rho^{-1}) \ll 1$ ) even if both initial partons are on-shell,  $p_1^2 \approx p_2^2 \approx 0$ , as relevant for electroweak instanton-induced processes in proton-proton scattering at VLHC (cf. Fig. 1 (left)).

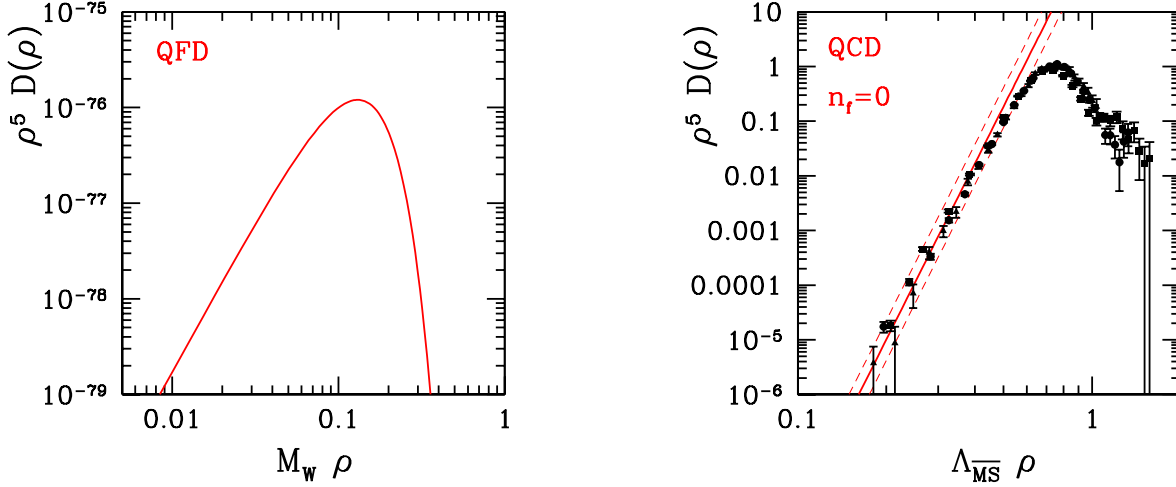


Figure 2: Instanton-size distributions as predicted in instanton-perturbation theory (solid lines) in QFD (left) and quenched ( $n_f = 0$ ) QCD (right). Both display a powerlike decrease,  $\rho^5 D(\rho) \propto \rho^{\beta_0}$ , towards decreasing sizes due to asymptotic freedom, with  $\beta_0 = 19/6$  for QFD and  $\beta_0 = 11$  for quenched QCD. For QCD (right), the two-loop renormalization group invariant prediction for the size distribution from Ref. [39] together with the 3-loop form of  $\alpha_{\overline{\text{MS}}}$ , with  $\Lambda_{\overline{\text{MS}}}^{(0)} = 238 \pm 19$  MeV from the ALPHA collaboration [42], was used. The error band (dashed lines) results from the errors in  $\Lambda_{\overline{\text{MS}}}$  and a variation of  $\mu = 1 \div 10$  GeV. *Left:* Towards large sizes,  $\rho > \rho_{\text{max}} = 0.13/M_W$ , the QFD instanton size distribution decreases exponentially due to the Higgs mechanism. *Right:* For large sizes,  $\Lambda_{\overline{\text{MS}}} \rho \gtrsim 0.75$ , the QCD instanton size distribution, as determined from recent high-quality lattice data from UKQCD [27]<sup>2</sup>, appears to decrease exponentially,  $\propto \exp(-c\rho^2)$  [22, 47], similar to the QFD size distribution (left), but unlike the instanton-perturbative prediction (solid). For  $\Lambda_{\overline{\text{MS}}} \rho \lesssim 0.42$ , on the other hand, one observes a remarkable agreement with the predictions from instanton-perturbation theory (solid) [22, 24].

In QCD, on the other hand, the perturbative expression (5) for the size distribution has a power-law behavior,  $\propto \rho^{\beta_0-5}$  (cf. Fig. 2 (right)). The latter generically causes the dominant contributions to observables like the cross-section (2) to originate from large  $\rho \sim \Lambda^{-1} \Rightarrow \alpha_s(\rho^{-1}) \sim 1$  and thus often spoils the applicability of instanton-perturbation theory. Deep-inelastic scattering, however, offers a unique possibility to probe the predictions of instanton-perturbation theory [20, 21, 22, 23, 24]. This can be understood as follows. In deep-inelastic electron-proton scattering, the virtual photon splits into a quark and an antiquark, one of which,  $p_1$  say, enters the instanton subprocess (cf. Fig. 1 (right)). This parton carries a space-like virtuality  $\hat{Q}^2 \equiv -p_1^2 \geq 0$ , which can be made very large by kinematical cuts on the final state. In this case the contribution of large instantons to the integrals is suppressed by the exponential form factors (4) in expression (2),  $\propto e^{-\hat{Q}(\rho+\bar{\rho})}$ , and instanton-perturbation theory becomes exploitable, i.e. predictive [20, 21]. In this connection it is quite welcome that lattice data on the instanton content of the quenched ( $n_f = 0$ ) QCD vacuum [27]<sup>2</sup> can be used to infer the region of validity of instanton-perturbation theory for  $D(\rho)$  [22, 24]: As illustrated in Fig. 2 (right), there is very good agreement for  $\Lambda_{\overline{\text{MS}}} \rho \lesssim 0.42$ .

<sup>2</sup>For further, qualitative similar lattice data, see Refs. [43, 44] and the reviews [45, 46].

*Ad ii)* A second important building block of the cross-section (2) is the function  $\Omega(U, R^2/(\rho\bar{\rho}), \bar{\rho}/\rho)$ , appearing in the exponent with a large numerical coefficient  $4\pi/\alpha_g$ . It incorporates the effects of final-state (gauge) bosons, mainly  $W$ 's and  $Z$ 's in the case of QFD and gluons in the case of QCD. Within strict instanton-perturbation theory, it is given in form of a perturbative expansion [12, 37, 21] for large  $I\bar{I}$ -distance  $R^2$ . Beyond this expansion, one may identify  $\Omega$  with the interaction between an instanton and an anti-instanton, which may be systematically evaluated by means of the so-called  $I\bar{I}$ -valley method [35]. The corresponding interaction has been found analytically for the case of pure  $SU(2)$  gauge theory<sup>3</sup> [13, 36],

$$\Omega_g = \Omega_0 + \Omega_1 u_0^2 + \Omega_2 u_0^4, \quad (9)$$

with

$$\begin{aligned} \Omega_0 &= 2 \frac{z^4 - 2z^2 + 1 + 2(1 - z^2) \ln z}{(z^2 - 1)^3}, \\ \Omega_1 &= -8 \frac{z^4 - z^2 + (1 - 3z^2) \ln z}{(z^2 - 1)^3}, \\ \Omega_2 &= -16 \frac{z^2 - 1 - (1 + z^2) \ln z}{(z^2 - 1)^3}. \end{aligned} \quad (10)$$

Due to conformal invariance of classical pure Yang-Mills theory, it depends on the sizes  $\rho$ ,  $\bar{\rho}$ , and the  $I\bar{I}$ -distance  $R$  only through the “conformal separation”,

$$z = \frac{1}{2} \left( \xi + \sqrt{\xi^2 - 4} \right), \quad \xi = \frac{R^2}{\rho\bar{\rho}} + \frac{\bar{\rho}}{\rho} + \frac{\rho}{\bar{\rho}} \geq 2, \quad (11)$$

and on the relative color orientation<sup>3</sup>  $U = u_0 + i\sigma^k u_k$ , with  $u_0^2 + u^k u_k = 1$ , only through  $u_0$ .

Note that  $I\bar{I}$ -pairs with the most attractive relative orientation,  $U = 1$ , give the dominant contribution to the cross-section (2) in the weak coupling regime,  $\alpha_g \ll 1$ . For this relative orientation, the  $I\bar{I}$ -valley represents a gauge field configuration of steepest descent interpolating between an infinitely separated  $I\bar{I}$ -pair, corresponding to twice the instanton action,  $S^{(I\bar{I})} = 2[1 + \Omega_g(U = 1, \xi = \infty)] = 2$ , and a strongly overlapping one, annihilating to the perturbative vacuum at  $\xi = 2$  ( $R = 0, \rho = \bar{\rho}$ ), corresponding to vanishing action  $S^{(I\bar{I})} = 2[1 + \Omega_g(U = 1, \xi = 2)] = 0$  (cf. Fig. 3 (left)). It is thus clear that near  $\xi \approx 2$  the semi-classical approximation based on the  $I\bar{I}$ -valley breaks down and no reliable non-perturbative information can be extracted from it.

Here again high-quality lattice data [27] on the  $I\bar{I}$ -distance distribution in quenched QCD allow to estimate the fiducial region in  $\xi$  or more specifically in  $R/\langle\rho\rangle$ , where  $\langle\rho\rangle \approx 0.5$  fm is the average instanton/anti-instanton size measured on the lattice (cf. Fig. 2 (right)). One finds good agreement with the predictions from instanton-perturbation theory for  $R/\langle\rho\rangle \gtrsim 1.0 \div 1.05$  [22, 24] (cf. Fig. 3 (right)). In this case, however, there are remaining ambiguities. *a)* The integrations over  $\rho$ ,  $\bar{\rho}$  in the  $I\bar{I}$ -distance distribution  $dn_{I\bar{I}}/(d^4x d^4R)$  imply significant contributions also from larger instantons with  $0.42 \lesssim \Lambda_{\overline{\text{MS}}} \rho, \Lambda_{\overline{\text{MS}}} \bar{\rho} \lesssim 1$ , outside the region of instanton-perturbation theory. A

---

<sup>3</sup>For the embedding of the  $SU(2)$   $I\bar{I}$ -valley into  $SU(3)$ , see e.g. Ref. [22].

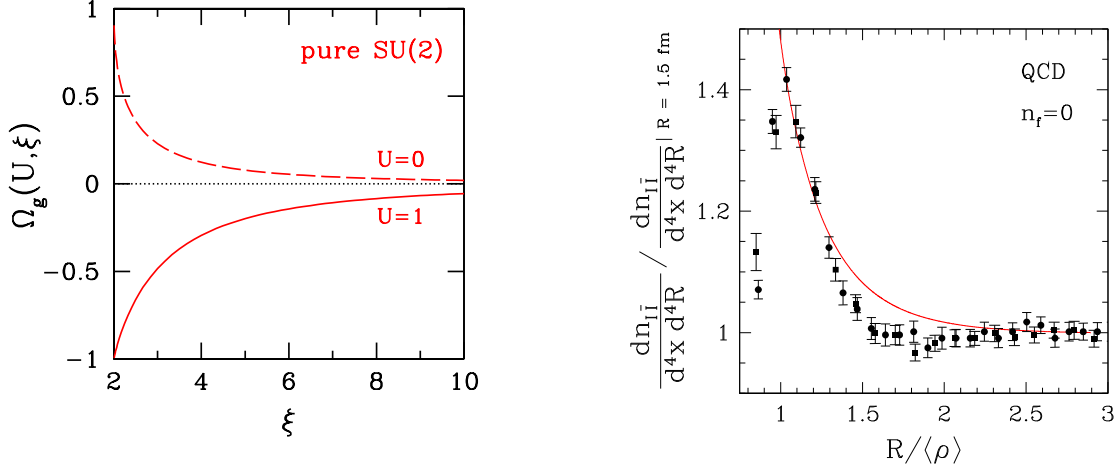


Figure 3: *Left:*  $I\bar{I}$ -valley interaction (9) as function of conformal separation  $\xi$  (11) for the most attractive relative orientation ( $U = 1$ , solid) and the most repulsive relative orientation ( $U = 0$ , dashed). *Right:* Illustration of the agreement of recent high-quality lattice data [27] for the  $I\bar{I}$ -distance distribution with the predictions from instanton-perturbation theory (solid) for  $R/\rho \gtrsim 1.05$  [22, 24].

more differential lattice measurement of the distance distribution,  $dn_{I\bar{I}}/(d^4x d^4R d\rho d\bar{\rho})$ , which includes also differentials with respect to the sizes  $\rho$  and  $\bar{\rho}$ , and eventually a test of its conformal properties would resolve these theoretical ambiguities. *b)* Furthermore, at small  $I\bar{I}$ -separation  $R < (\rho + \bar{\rho})/2$ , the extraction of the  $I\bar{I}$ -distance distribution from the quenched QCD lattice data is quite ambiguous since there is no principal distinction between a trivial gauge field fluctuation and an  $I\bar{I}$ -pair at small separation. This is reflected in a considerable dependence on the cooling method/amount used to infer properties of the  $I\bar{I}$ -distance distribution [44, 46]. A simple extrapolation of lattice results on the topological structure of quenched  $SU(2)$  gauge theory [44] to zero “cooling radius” indicates  $\langle R/(\rho + \bar{\rho})/2 \rangle \approx 0.5$ , i.e. strongly overlapping  $I\bar{I}$ -pairs in the vacuum, unlike Fig. 3 (right). Therefore, the fiducial region  $R^2/(\rho\bar{\rho}) \geq 1$  for the reliability of instanton-perturbation theory inferred from lattice data should be considered as quite conservative.

*Ad iii)* Finally, as the last important building block of (2), let us just quote the result from Ref. [21] for the fermionic overlap integral  $\omega$  [14] in the most attractive relative orientation,  $U = 1$ ,

$$\omega = \frac{3\pi}{8} \frac{1}{z^{3/2}} {}_2F_1\left(\frac{3}{2}, \frac{3}{2}; 4; 1 - \frac{1}{z^2}\right). \quad (12)$$

3. In the weak-coupling regime,  $\alpha_g \ll 1$ , the collective coordinate integrals in the cross-section (2) can be performed in the saddle-point approximation, where the relevant effective exponent reads<sup>4</sup>

$$-\Gamma \equiv i(p_1 + p_2) \cdot R \quad (13)$$

<sup>4</sup>In the case of QCD, some additional terms, which arise from the running of  $\alpha_s$  and are formally of pre-exponential nature, have to be included in Eqs. (13) and (14) for numerical accuracy [21]. In this letter, we adopt the simplified expressions (13), (14) which suffice for illustrative purposes and are numerically adequate for QFD.

$$- \begin{cases} \frac{4\pi}{\alpha_W(\mu)} \left[ 1 + \frac{1}{4} M_W^2 (\rho^2 + \bar{\rho}^2) + \Omega_g \left( U, \frac{R^2}{\rho\bar{\rho}}, \frac{\bar{\rho}}{\rho} \right) \right] & \text{in QFD } (p_1^2 = p_2^2 = 0), \\ \hat{Q}(\rho + \bar{\rho}) + \frac{4\pi}{\alpha_s(\mu)} \left[ 1 + \Omega_g \left( U, \frac{R^2}{\rho\bar{\rho}}, \frac{\bar{\rho}}{\rho} \right) \right] & \text{in QCD (DIS: } -p_1^2 = \hat{Q}^2 > 0, p_2^2 = 0). \end{cases}$$

For the case of QFD, we have neglected in (13) the Higgs part  $\Omega_h$  of the  $I\bar{I}$ -interaction and took for the gauge part the one from the pure gauge theory,  $\Omega_g$ . This should be reliable as long as the dominant contribution to the QFD instanton-induced cross-section is due to the multiple production of transverse  $W$ 's and  $Z$ 's – as is the case at energies below the sphaleron (1) – rather than of longitudinal ones and of Higgs bosons [13]. The saddle-point equations,  $\partial\Gamma/\partial\chi|_{\chi_*} = 0$ , with  $\chi = \{U, R, \rho, \bar{\rho}\}$ , following from (13) imply  $U_* = 1$ ,  $\rho_* = \bar{\rho}_*$ , and can be summarized as<sup>4</sup>

$$\begin{cases} \left( \frac{R}{\rho} \right)_* = M_W \rho_* \left( \frac{4\pi M_W / \alpha_W}{\sqrt{\hat{s}}} \right), \quad \frac{1}{2} (M_W \rho_*)^2 = \left[ (\xi_* - 2) \frac{\partial}{\partial \xi_*} \Omega_g(1, \xi_*) \right]_{|\xi_* = 2 + (\frac{R}{\rho})_*^2} & \text{in QFD}, \\ \left( \frac{R}{\rho} \right)_* = 2 \frac{\hat{Q}}{\sqrt{\hat{s}}}, \quad \hat{Q} \rho_* = \frac{4\pi}{\alpha_s} \left[ (\xi_* - 2) \frac{\partial}{\partial \xi_*} \Omega_g(1, \xi_*) \right]_{|\xi_* = 2 + (\frac{R}{\rho})_*^2} & \text{in QCD}, \end{cases} \quad (14)$$

where  $(p_1 + p_2)^2 = \hat{s}$  denotes the parton-parton center-of-mass (cm) energy. To exponential accuracy, the cross-section (2) is then given by

$$\hat{\sigma}^{(I)} \propto e^{-\Gamma_*} \equiv e^{-\frac{4\pi}{\alpha_g} F_g(\epsilon)}, \quad (15)$$

where

$$\epsilon = \begin{cases} \frac{\sqrt{\hat{s}}}{4\pi M_W / \alpha_W} & \text{in QFD}, \\ \frac{\sqrt{\hat{s}}}{\hat{Q}} & \text{in QCD}, \end{cases} \quad (16)$$

$$F_g = \begin{cases} \left[ 1 + \Omega_g(1, \xi_*) - (\xi_* - 2) \frac{\partial}{\partial \xi_*} \Omega_g(1, \xi_*) \right]_{|\xi_* = 2 + (\frac{R}{\rho})_*^2} & \text{in QFD}, \\ \left[ 1 + \Omega_g(1, \xi_*) \right]_{|\xi_* = 2 + (\frac{R}{\rho})_*^2} & \text{in QCD}. \end{cases} \quad (17)$$

Both in QFD as well as in QCD, the prediction (17) for the “holy-grail function [17]”  $F_g(\epsilon)$  decreases monotonically for increasing scaled energy  $\epsilon$  from  $F_g(0) = 1$ . It approaches zero,  $F_g \rightarrow 0$ , at asymptotic energies,  $\epsilon \rightarrow \infty$  (cf. Fig. 4 (middle)). Thus, at all finite energies, the cross-section (15) is formally exponentially suppressed and there is no apparent problem with unitarity [7]. On the other hand, it is seen that at high cm energies the  $I\bar{I}$ -interaction is probed at small distances,  $(R/\rho)_* \sim 1$  (cf. Fig. 4 (top)), making the semi-classical and saddle-point evaluation unreliable. In this connection, the information on the fiducial region in  $R/\langle\rho\rangle$  of the instanton-perturbative description from QCD lattice simulations (cf. Fig. 3 (right)) can be most appreciated. Note furthermore that, in the case of QFD,  $M_W R_* \lesssim 1$  in the whole energy range considered in Fig. 4 (top), justifying a posteriori the approximation of the full valley interaction in QFD by the one from the pure gauge theory,  $\Omega_g$ .

Further information on the fiducial region in  $(R/\rho)_*$  may be obtained from DIS experiments at HERA. Meanwhile, the results of a first dedicated search for QCD instanton-induced processes in DIS have been published by the H1 collaboration [25]. In this study, the theory and phenomenology of hard QCD instanton-induced processes in DIS developed by Fridger Schrempp and myself [19, 20, 21, 22, 23, 24] has been used heavily. Several observables characterising the



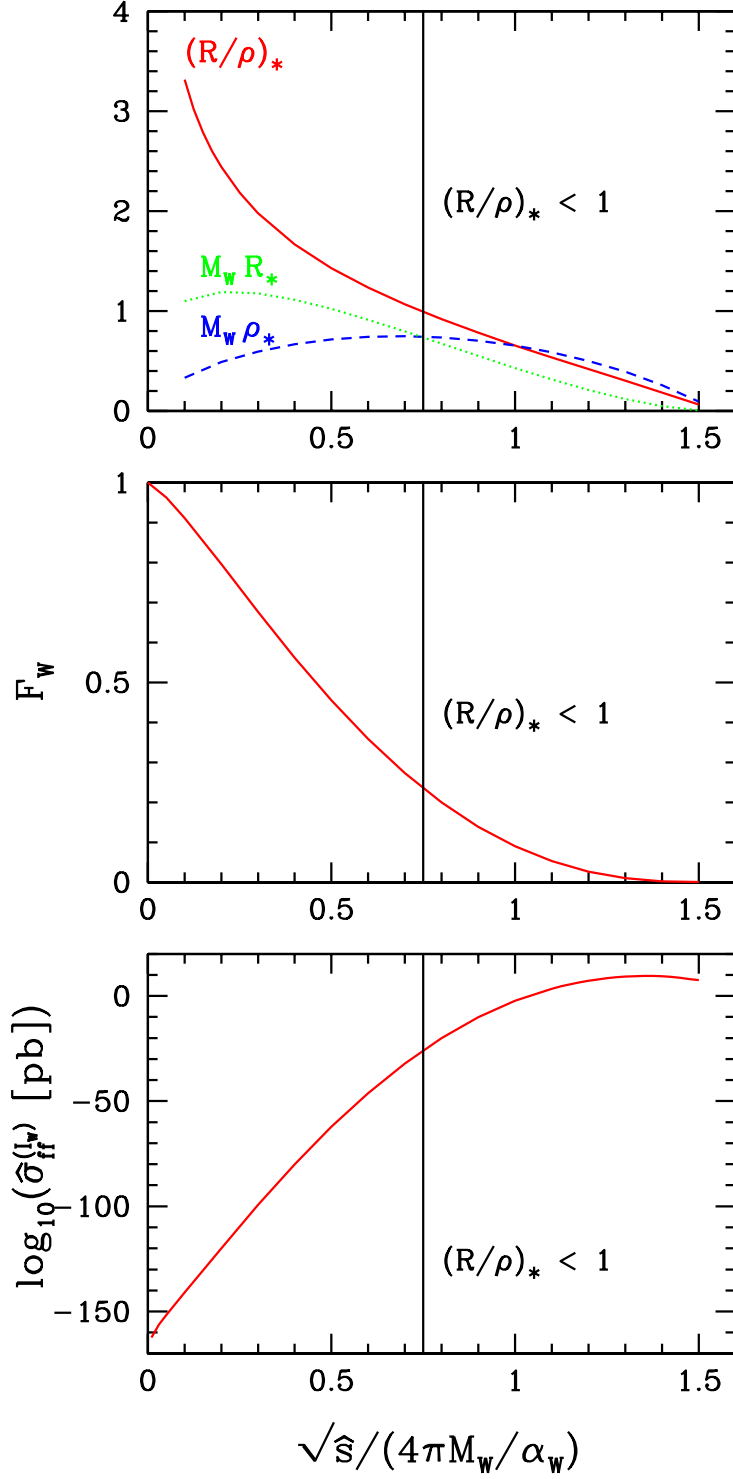


Figure 4: QFD instanton subprocess cross-section related quantities, as function of scaled parton-parton center-of-mass energy  $\sqrt{\hat{s}}/(4\pi M_W/\alpha_W)$ . *Top*: Saddle point values for collective coordinates [13]. *Middle*: Holy-grail function,  $\hat{\sigma}^{(I_W)} \propto \exp[-(4\pi/\alpha_W) F_W]$  [13]. *Bottom*: Total cross-section  $\hat{\sigma}_{ff}^{(I_W)}$  for QFD instanton-induced fermion-fermion scattering,  $f + f \xrightarrow{I_W} \text{all}$ .

hadronic final state of QCD instanton-induced events were exploited to identify a potentially instanton-enriched domain. The results obtained are intriguing but non-conclusive. While an excess of events with instanton-like topology over the expectation of the standard DIS background is observed, which, moreover, is compatible with the instanton-signal, it can not be claimed to be significant given the uncertainty of the Monte Carlo simulations of the standard DIS background. Therefore, only upper limits on the cross-section for QCD instanton-induced processes are set, dependent on the kinematic domain considered [25]. From this analysis one may infer, via the saddle point correspondence, that the cross-section calculated within instanton-perturbation theory is ruled out for  $(R/\rho)_* \lesssim 0.84$ , in a range  $0.31 \text{ fm} \lesssim \rho_* \lesssim 0.33 \text{ fm}$  of effective instanton sizes. One should note, however, that in the corresponding – with present statistics accessible – kinematical range the running coupling is quite large,  $\alpha_s(\rho_*^{-1}) \approx 0.4$ , and one is therefore not very sensitive<sup>5</sup> to the  $I\bar{I}$ -interaction, which appears in the exponent with coefficient  $4\pi/\alpha_s \approx 31$ . This should be contrasted with QFD, which is extremely sensitive to  $\Omega$ , since  $4\pi/\alpha_W \approx 372$ . An extension of the present H1 limit on  $(R/\rho)_*$  towards smaller  $\rho_*$  and  $\alpha_s(\rho_*^{-1})$ , which should be possible with increased statistics at HERA II, would be very welcome. At present, the data do not exclude the cross-section predicted by instanton-perturbation theory for small  $(R/\rho)_* \gtrsim 0.5$ , as long as one probes only very small instanton-sizes  $\rho_* \ll 0.3 \text{ fm}$ .

4. Finally, let us present the result of a state of the art evaluation of the cross-section (2) for QFD, including all the prefactors – an analogous evaluation has been presented for DIS in QCD in Ref. [21]. For the case of fermion-fermion scattering via QFD instantons/sphalerons, as relevant at VLHC at the parton level, we find

$$\begin{aligned}
M_W^2 \hat{\sigma}_{\text{ff}}^{(I_W)} &= \frac{\pi^{15/2}}{128} d_{\text{MS}}^2 \left( \frac{4\pi}{\alpha_W(\mu)} \right)^{7/2} (\mu \rho_*)^{2\beta_0} \\
&\times (\omega(\xi_*))^{10} \frac{1}{\sqrt{\xi_* \left( \frac{\partial^2}{\partial \xi_*^2} \Omega_g(1, \xi_*) \right) \left( \frac{\partial}{\partial \xi_*} \Omega_g(1, \xi_*) \right)^3 (\Omega_1(\xi_*) + 2 \Omega_2(\xi_*))^3}} \\
&\times \exp \left[ -\frac{4\pi}{\alpha_W(\mu)} \left( 1 + \Omega_g(1, \xi_*) - (\xi_* - 2) \frac{\partial}{\partial \xi_*} \Omega_g(1, \xi_*) \right) \right] \Big|_{\xi_* = 2 + \left( \frac{R}{\rho} \right)_*^2},
\end{aligned} \tag{18}$$

expressed entirely in terms of the solutions of the saddle-point equations (14). The various factors in Eq. (18) can be easily understood. The ones in the first line are mainly due to the square of the size distribution (5), taken at the saddle-point. The power of  $(4\pi/\alpha_W)$  is reduced here from nominally  $4N_c = 8$  to  $7/2$ , because there are effectively 9 saddle-point integrals giving rise – apart from the square-root factor in the second line of Eq. (18) – to a factor of  $(4\pi/\alpha_W)^{-9/2}$ . The explicit factor of  $1/(2p_1 \cdot p_2) = 1/\hat{s}$  in Eq. (2) does not appear in Eq. (18), because it is cancelled by another explicit energy dependence in the factor  $\mathcal{P}_{\text{ff}}^W|_* = 8\pi^4 \rho_*^6 \hat{s}$ . Finally, the last line in Eq. (18) is just the main exponential (15),  $e^{-\Gamma^*}$ .

The prediction<sup>6</sup> (18) for the QFD instanton-induced fermion-fermion cross-section is displayed

<sup>5</sup>This is of course welcome for the QCD-instanton searches at HERA, because it makes predictions for the bulk of data quite reliable.

<sup>6</sup>At  $\epsilon \sim 1$  it should be rather called an educated extrapolation or guess.

in Fig. 4 (bottom) as a function of the scaled fermion-fermion cm energy  $\epsilon = \sqrt{s}/(4\pi M_W/\alpha_W)$ , for a choice  $\mu = M_W$  of the renormalization scale. In the strict region of instanton-perturbation theory,  $\epsilon \ll 1$ , the cross-section is really tiny, e.g.  $\hat{\sigma}_{\text{ff}}^{(I_W)} \approx 10^{-141}$  pb at  $\epsilon \approx 0.1$ , but steeply growing. Nevertheless, it is expected to be unobservably small,  $\hat{\sigma}_{\text{ff}}^{(I_W)} \lesssim 10^{-26}$  pb for  $\epsilon \lesssim 0.75$ , in the conservative fiducial kinematical region corresponding to  $(R/\rho)_* \gtrsim 1$  inferred via the QFD–QCD analogy from lattice data and HERA. If we allow, however, for a slight extrapolation towards smaller  $(R/\rho)_* \approx 0.7$  – still compatible with lattice results and HERA – the prediction<sup>6</sup> rises to  $\hat{\sigma}_{\text{ff}}^{(I_W)} \approx 10^{-6}$  pb at  $\epsilon \approx 1$ , corresponding to a parton-parton cm energy of about 30 TeV. In this case, QFD instanton-induced  $B + L$  violating events will have observable rates at VLHC, which has a projected proton-proton cm energy of  $\sqrt{s} = 200$  TeV and a luminosity of about  $\mathcal{L} \approx 6 \cdot 10^5 \text{ pb}^{-1} \text{ yr}^{-1}$  [29], and an exciting phenomenology will emerge [15]. If we assume the prediction<sup>6</sup> (18) to be valid even at higher energies, corresponding to even smaller  $(R/\rho)_*$ , than we can expect to be able to see the first signs of electroweak sphaleron production in present day or near future cosmic ray facilities and neutrino telescopes [16], even before the commissioning of VLHC. In the meantime, we can try to improve our knowledge about QCD instantons on the lattice and in deep-inelastic scattering at HERA, with important implications also for QFD instantons at very high energies.

## Acknowledgements

I would like to thank F. Schrempp for many fruitful discussions and a careful reading of the manuscript. Furthermore, I would like to thank the organizers of the 26th Johns Hopkins Workshop on Current Problems in Particle Theory, Heidelberg, August 1-3, 2002, in particular O. Nachtmann, for inspiration and encouragement of the present work.

## References

- [1] S. L. Adler, Phys. Rev. **177** (1969) 2426; J. S. Bell and R. Jackiw, Nuovo Cim. A **60** (1969) 47; W. A. Bardeen, Phys. Rev. **184** (1969) 1848.
- [2] G. 't Hooft, Phys. Rev. Lett. **37** (1976) 8; Phys. Rev. D **14** (1976) 3432 [Erratum-ibid. D **18** (1978) 2199].
- [3] A. Belavin, A. Polyakov, A. Shvarts and Y. Tyupkin, Phys. Lett. B **59** (1975) 85.
- [4] E. V. Shuryak, Nucl. Phys. B **203** (1982) 93; D. Diakonov and V. Y. Petrov, Phys. Lett. B **147** (1984) 351; Nucl. Phys. B **272** (1986) 457.
- [5] T. Schäfer and E. V. Shuryak, Rev. Mod. Phys. **70** (1998) 323; H. Forkel, arXiv:hep-ph/0009136; D. Diakonov, arXiv:hep-ph/0212026.
- [6] V. A. Kuzmin, V. A. Rubakov and M. E. Shaposhnikov, Phys. Lett. B **155** (1985) 36; P. Arnold and L. D. McLerran, Phys. Rev. D **36** (1987) 581; A. Ringwald, Phys. Lett. B **201** (1988) 510.

- [7] V. A. Rubakov and M. E. Shaposhnikov, Usp. Fiz. Nauk **166** (1996) 493 [Phys. Usp. **39** (1996) 461].
- [8] A. Ringwald, to appear in *QCD02*, Montpellier, France, 2002, arXiv:hep-ph/0210209.
- [9] H. Aoyama and H. Goldberg, Phys. Lett. B **188** (1987) 506.
- [10] A. Ringwald, Nucl. Phys. B **330** (1990) 1; O. Espinosa, Nucl. Phys. B **343** (1990) 310.
- [11] L. D. McLerran, A. I. Vainshtein and M. B. Voloshin, Phys. Rev. D **42** (1990) 171; J. M. Cornwall, Phys. Lett. B **243** (1990) 271; P. B. Arnold and M. P. Mattis, Phys. Rev. D **42** (1990) 1738; S. Y. Khlebnikov, V. A. Rubakov and P. G. Tinyakov, Nucl. Phys. B **347** (1990) 783; *ibid.* B **350** (1991) 441; A. H. Mueller, Nucl. Phys. B **348** (1991) 310; *ibid.* B **353** (1991) 44; A. Ringwald and C. Wetterich, Nucl. Phys. B **353** (1991) 303; M. Maggiore and M. A. Shifman, Nucl. Phys. B **371** (1992) 177; V. V. Khoze, J. Kripfganz and A. Ringwald, Phys. Lett. B **275** (1992) 381 [Erratum-*ibid.* B **279** (1992) 429]; *ibid.* B **277** (1992) 496; A. Ringwald, Phys. Lett. B **285** (1992) 113; V. A. Rubakov, D. T. Son and P. G. Tinyakov, Phys. Lett. B **287** (1992) 342; D. Diakonov and V. Petrov, Phys. Rev. D **50** (1994) 266; F. Bezrukov, C. Rebbi, V. Rubakov and P. Tinyakov, arXiv:hep-ph/0110109.
- [12] V. I. Zakharov, Nucl. Phys. B **371** (1992) 637; M. Porrati, Nucl. Phys. B **347** (1990) 371; V. V. Khoze and A. Ringwald, Nucl. Phys. B **355** (1991) 351.
- [13] V. V. Khoze and A. Ringwald, Phys. Lett. B **259** (1991) 106.
- [14] E. V. Shuryak and J. J. Verbaarschot, Phys. Rev. Lett. **68** (1992) 2576.
- [15] G. R. Farrar and R.-b. Meng, Phys. Rev. Lett. **65** (1990) 3377; A. Ringwald, F. Schrempp and C. Wetterich, Nucl. Phys. B **365** (1991) 3; M. J. Gibbs, A. Ringwald, B. R. Webber and J. T. Zadrozny, Z. Phys. C **66** (1995) 285; M. J. Gibbs and B. R. Webber, Comput. Phys. Commun. **90** (1995) 369.
- [16] D. A. Morris and R. Rosenfeld, Phys. Rev. D **44** (1991) 3530; D. A. Morris and A. Ringwald, Astropart. Phys. **2** (1994) 43.
- [17] M. P. Mattis, Phys. Rept. **214** (1992) 159; P. G. Tinyakov, Int. J. Mod. Phys. A **8** (1993) 1823; R. Guida, K. Konishi and N. Magnoli, Int. J. Mod. Phys. A **9** (1994) 795.
- [18] I. I. Balitsky and V. M. Braun, Phys. Lett. B **314** (1993) 237.
- [19] A. Ringwald and F. Schrempp, in *Quarks '94*, Vladimir, Russia, 1994, arXiv:hep-ph/9411217.
- [20] S. Moch, A. Ringwald and F. Schrempp, Nucl. Phys. B **507** (1997) 134.
- [21] A. Ringwald and F. Schrempp, Phys. Lett. B **438** (1998) 217.
- [22] A. Ringwald and F. Schrempp, Phys. Lett. B **459** (1999) 249.
- [23] A. Ringwald and F. Schrempp, Comput. Phys. Commun. **132** (2000) 267.

- [24] A. Ringwald and F. Schrempp, Phys. Lett. B **503** (2001) 331.
- [25] C. Adloff *et al.* [H1 Collaboration], Eur. Phys. J. C **25** (2002) 495.
- [26] D. E. Kharzeev, Y. V. Kovchegov and E. Levin, Nucl. Phys. A **690** (2001) 621; M. A. Nowak, E. V. Shuryak and I. Zahed, Phys. Rev. D **64** (2001) 034008; F. Schrempp, J. Phys. G **28** (2002) 915; F. Schrempp and A. Utermann, Phys. Lett. B **543** (2002) 197.
- [27] D. A. Smith and M. J. Teper [UKQCD collaboration], Phys. Rev. D **58** (1998) 014505.
- [28] The Eurasian Long Intersecting Storage Ring (ELOISATRON), <http://emcsc.ccsem.infn.it/ELN.html>
- [29] The Very Large Hadron Collider (VLHC), <http://www.vlhc.org>
- [30] I. Affleck, Nucl. Phys. B **191** (1981) 429.
- [31] R. Jackiw and C. Rebbi, Phys. Rev. Lett. **37** (1976) 172; C. G. Callan, R. F. Dashen and D. J. Gross, Phys. Lett. B **63** (1976) 334.
- [32] F. R. Klinkhamer and N. S. Manton, Phys. Rev. D **30** (1984) 2212.
- [33] F. R. Klinkhamer, Nucl. Phys. B **376** (1992) 255; *ibid.* B **407** (1993) 88.
- [34] I. I. Balitsky and V. M. Braun, Phys. Rev. D **47** (1993) 1879.
- [35] A. V. Yung, Nucl. Phys. B **297** (1988) 47.
- [36] J. J. Verbaarschot, Nucl. Phys. B **362** (1991) 33 [Erratum-*ibid.* B **386** (1992) 236].
- [37] P. B. Arnold and M. P. Mattis, Phys. Rev. D **44** (1991) 3650; A. H. Mueller, Nucl. Phys. B **364** (1991) 109; D. Diakonov and V. Petrov, in *26th LNPI Winter School*, Leningrad, 1991, pp. 8-64; D. Diakonov and M. V. Polyakov, Nucl. Phys. B **389** (1993) 109; I. Balitsky and A. Schäfer, Nucl. Phys. B **404** (1993) 639.
- [38] C. W. Bernard, Phys. Rev. D **19** (1979) 3013.
- [39] T. R. Morris, D. A. Ross and C. T. Sachrajda, Nucl. Phys. B **255** (1985) 115.
- [40] K. Hagiwara *et al.* [Particle Data Group Collaboration], Phys. Rev. D **66** (2002) 010001.
- [41] A. Hasenfratz and P. Hasenfratz, Nucl. Phys. B **193** (1981) 210; M. Lüscher, Nucl. Phys. B **205** (1982) 483; G. 't Hooft, Phys. Rept. **142** (1986) 357.
- [42] S. Capitani, M. Lüscher, R. Sommer and H. Wittig [ALPHA Collaboration], Nucl. Phys. B **544** (1999) 669 [arXiv:hep-lat/9810063].
- [43] A. Hasenfratz and C. Nieter, Phys. Lett. B **439** (1998) 366.
- [44] M. Garcia Perez, O. Philipsen and I. O. Stamatescu, Nucl. Phys. B **551** (1999) 293.

- [45] J. W. Negele, Nucl. Phys. Proc. Suppl. **73** (1999) 92; M. Teper, Nucl. Phys. Proc. Suppl. **83** (2000) 146.
- [46] I. O. Stamatescu, arXiv:hep-lat/0002005.
- [47] E. V. Shuryak, arXiv:hep-ph/9909458.